ISSN 2348-313X (Print)
International Journal of Life Sciences Research ISSN 2348-3148 (online)
Vol. 4, Issue 2, pp: (253-262), Month: April - June 2016, Available at: www.researchpublish.com

In Silico identification of lead compounds for the inhibition of *Mycobacterium tuberculosis* IspE using complex based pharmacophore mapping, virtual screening and molecular dynamics simulation

[1]Eman Abdullah Almuqri, [2]Mohammad Teimouri, [3]Junaid Muhammad

[1,2,3]Department of Biotechnology, College of Life Science and Technology,
Huazhong University of Science and Technology, 1037 Luoyu Rd., Wuhan 430074, Hubei

Abstract: **IspE contributes to the fourth step of non-mevalonate pathway in *Mycobacterium tuberculosis* and other pathogenic species. The non-mevalonate pathway is engaged in the synthesis of isoprenoid precursor. The precursors of the isoprenoids are the isopentenyl diphosphate (IPP) and dimethylallyl pyrophosphate (DMAPP). IspE catalyzes the transfer of γ-phosphoryl group from ATP to 4-diphosphocytidyl-2C-methyl-d-erythritol (CDP-ME) resulting in 4-diphosphocytidyl-2C-methyl-D-erythritol-2-phosphate (CDP-ME2P). Based on the crystal structure of IspE complex with AMP-PNP from *Mycobacterium tuberculosis*, the virtual screening was carried out using ZINC database. The pharmacophore model was developed based on the AMP-PNP interactions with IspE. A subset of 5805 molecules was extracted from ZINC database utilizing the developed pharmacophore model. Through the docking and binding affinity approach, five novel compounds were identified that may act as inhibitors of IspE. Further, the molecular dynamics simulation (MD simulation) revealed that four compounds (compound 1, 2, 3 and 4) among them are more stable in the active site. The MMPBSA analysis also supports the four compounds as good inhibitors in term of binding energy. More interestingly, these compounds show diversity in their structure and also show no resemblance with other published inhibitors. As these compounds belong to the different class of compound, this study is providing an opportunity to further synthesize the derivatives of each compound for the optimization of their inhibitory activity. Therefore, in the present study, five compounds were described as a novel lead compounds that will act as good starting point for the drug discovery.**

Keyword: **IspE Inhibitors, Molecular docking, MD Simulation, ZINC database, MMPBSA analysis, *Mycobacterium tuberculosis.***

I. INTRODUCTION

Mycobacterium tuberculosis, one of the widespread human pathogen, is responsible for the total of 1.6 million deaths every year. More-ever, it infects approximately 10 million peoples every year. Unfortunately, this condition become more worst due to poor living conditions and the emergence of multidrug-resistant (MDR) and extensively drug-resistant (XDR) Mycobacterium tuberculosis strains [1]. Despite improvements and developments with supervised administration of rifampin, pyrazinamide and isoniazid drug regimen [2], tuberculosis (TB) remains one of the most prevalent infectious diseases worldwide. Therefore, the identification of new drug targets is essential.

Isoprenoids, a hugely diverse group of molecules found in all organisms, contribute to the large group of natural products. The structurally diverse essential oils, components of macromolecules such as isopentenylated tRNAs and prenyl group, triterpenes, cannabinoids, sterols, dolichols, and ubiquinone are categorized as isoprenoids [3,4]. Isoprenoids play an important role in many physiological processes such as protein degradation, hormone-based signaling, meiosis, glycoprotein biosynthesis, hormone-based signaling and apoptosis.

The universal building blocks of the isoprenoid are the IPP and DMAPP [3,5-7]. Two different biosynthetic pathways for the synthesis of IPP and DMAPP are evolved, based on the organism's specific manner. In most eukaryotes, the precursors are synthesized through the mevalonate pathway [8-11]. In this pathway, the IPP is synthesized by three molecules of acetyl-CoA to 3-hydroxy-3-methylglutaryl-CoA followed by reduction, phosphorylation, and decarboxylation. Some of the IPP are isomerized to DMAPP. Most of the bacteria used the pathway in which the IPP and DMAPP synthesis is accompanied by deoxy-xylulose phosphate (DOXP) pathway, also called non-mevalonate pathway [3,11-13]. As the non-mevalonate pathway is absent in human and the enzymes involved in this pathway have no orthologous in human, therefore this pathway has been validated as a potential target for the structure based drug development [14]. Inhibition of the non-mevalonate pathway's enzymes has been validated as new approach for the drug development. Additionally, this pathway has been validated as a drug target by the fosmidomycin. Fosmidomycin has been known for its anti-malarial activity and it inhibit the the IspC of the non-mevalonate pathway [15]. Some of the IspE (Aquifex aeolicus) inhibitors of non-mevalonate pathways are also reported [4]. In the present study, the IspE from Mycobacterium tuberculosis was used for structured based drug screening.

The gene that encodes IspE is essential for the survival of Mycobacterium tuberculosis Escherichia coli, Haemophilus influenzae and Bacillus subtilis [16-18]. Crystal structure of IspE from Mycobacterium tuberculosis has been crystalized with its substrate CDP-ME and stable ATP analog AMP-PNP [19]. The structure shows distinct ATP and substrate binding site. Previous studies have been done for the drug designing, taking into account the substrate binding site of IspE [4,20]. The present study uses the ATP binding site for the screening of novel lead compound. Several studies for other proteins have been done that target the ATP binding sites [21-23]. In the present study, IspE from Mycobacterium tuberculosis was utilized for the screening purpose using ZINC commercial database. The combine approach of molecular docking and MD simulation was used to find the novel lead compound with diverse chemical structure that enables further optimization of lead compound.

II. MATERIAL AND METHODS

2.1 Structure-Based 3D Pharmacophore Generation

The pharmacophore tools implemented in MOE2014 determine chemical feature and their spatial arrangement in three dimensions that are important for the interaction. The X-ray crystal structure of IspE complex with AMP-PNP (PDB ID 3PYF) was used as an input file for the pharmacophore modeling. The important chemical features were identified based on the interaction of AMP-PNP with active site residues. The final pharmacophore model consists of four hydrogen bond acceptors and two hydrogen bond donors which were used for screening the ZINC database [24].

2.2 Database Screening

MOE generated pharmacopore model was used as template to search the chemical ZINC database for the purpose of finding novel and potential lead compounds. So with the aim of determining the novel lead compounds, the six features containing pharmacophore model generated by MOE was used as three dimensional queries for database search. As a result of this search, 5805 lead compound were obtained. Database screening offer the advantage that the lead compounds were easily available for testing than those based on de novo design method. If the molecule has to be hit, they must map the specified pharmacophoric features.

2.3 Molecular Docking

MOE-Dock program embedded in MOE2014 was used for docking. The crystal structure of the target protein was used for the docking study. Multiple conformations were generated for each ligand by applying a preferred torsion angles to all rotatable bonds in each ligand. Ten conformations were generated for each ligand. The accepted conformations for each ligand against receptor were scored using of London dG scoring function which calculates the free energy for the binding

of ligand from a given conformation. The final hits were docked using Autodock software to cross check and validate the results of MOE.

2.4 Binding Energy and Binding Affinity Calculations

To identify the most potential ligands, binding affinities of the hits-IspE complexes were calculated using Generalized-Born Volume Integral/Weighted Surface area method implemented in the MOE. Generalized Born interaction energy, such as Vander Waals, implicit solvent interaction energies and Coulomb electrostatic interaction, is non-bonded interaction energy between the receptor and the ligand molecule [25]. The binding affinity was calculated for each hit after energy minimization, and reported in unit of Kcal/Mol. The complexes having good affinity toward the IspE were further subjected to MD simulation to check its stability.

2.5 Dynamic Simulation

The MD simulation was carried out for each complex using amber14 software with ff14SB force field [26]. The system was made neutral by adding the Na+ counter ions. The complex structure was solvated with TIP3P water molecules in a rectangular box with 8.0 Å buffer distance along each side [27]. The accelerated GPU pmemd code was used to perform all steps of MD for each system [28]. Subsequently, the energy of the system was minimized in two steps using sander module of the amber14. First the energy of the water and counter ions was minimized keeping the protein fixed using harmonic constraint of strength of 500 kcal·mol^{-1}·Å^{-1}. Secondly, all atoms were energy minimized without restriction. In each step the steepest descent minimization of 2000 steps was followed by conjugate gradient minimization of 4000 steps. Then, the system was heated from 0 to 300 K in 500 ps and equilibrated at 300 K for another 500 ps. Finally, a 30 ns simulation without restriction was conducted at constant pressure and 300 K, and the coordinates were saved every 10,000 steps. During MD simulations, the SHAKE method was applied to constraint the covalent bonds involving hydrogen atom [29]. The Particle Mesh Ewald (PME) method was adopted to treat the long-range electrostatic interactions [30]. The cutoff distances for the long- range electrostatic and van der Waals interactions were set to 10.0 Å.

2.6 Binding Free Energy Analysis through MD simulation

The objective of the structure based drug designing approach is to find novel pharmaceutical compounds that bind to the drug target with good binding affinity [31,32]. Free energy calculations have become part of the standard repertoire of computational biochemical research due to their widespread applicability, reaching from the prediction of binding affinities of small drug-candidate compounds to the evaluation of relative stabilities of large bio-macromolecular structures. The MMPBSA.py script [33] was used to calculate the binding free energy of each compound within the active site of IspE based on the analysis of MD simulation trajectories. In the field of computational biology such as drug designing, the calculation of binding free energy has proven as a very useful tool.

III. RESULTS AND DISCUSSION

3.1 Pharmacophore Modeling and Virtual Screening

Complex-based pharmacophore modeling has an interesting application to determine the interaction points that may improve the binding affinity of the lead compound. A complex-based pharmacophore was developed on the basis of the crystal structure of Mycobacterium tuberculosis IspE complex with AMP-PNP (PDB ID 3PYF). The interactions of AMP-PNP with the active site of IspE were observed. The AMP-PNP binding site residues were defined as those within the 4 Å of AMP-PNP using Pymol software. Analysis of the IspE complex structure shows important residues that help in binding of AMP-PNP. The adeninyl moiety makes several hydrogen bonds with Asn70, Leu71 and Asp109. In addition the phosphate moiety makes hydrogen bonds with Ala100, Gly102, Gly105 and Gly106. The other residues such as Leu56, Leu64, Pro98, Val99, Gly101, Met103 and Ala104 are involved in hydrophobic interaction. While deriving pharmacophore model we aimed to keep a balance between complex pharmacophore which retrieve very potent compound but has only a very low hit rate and a relax pharmacophore which retrieve many compounds but with no activity. A total of six features including four hydrogen bond acceptors (Acc) and two hydrogen bond donors (Don) were included in the pharmacophore model. The aim of this pharmacophore modeling was to choose accurate lead compounds and to further search for the additional interactions with the active the site residues of IspE. The partial matching option in the pharmacophore modeling tool was set to five so, that the hit compounds match at least five features. The developed

pharmacophore model was used to screen the ZINC database.As a result of screening, 5805 compounds were retrieved as hits that match at least 5 features.

3.2 Molecular Docking and Binding Affinity Calculation

All the hit compounds were docked into the active site of IspE to explore the binding interactions of each hit compound inside the active site. The AMP-PNP was rescored in the active site of IspE and the score was found to be -4.83. The docking score of AMP-PNP was used as a cut off value to further screen the hit compounds. As compared to the docking score of AMP-PNP, 5805 molecules have good docking score. To identify the most potential ligands, the ligands having greater docking score than AMP-PNP were subjected to binding affinity calculation. The binding affinity of AMP-PNP was found to be -5.21kcal/mol. Fifteen molecules have good binding affinity that AMP-PNP. The fifteen compounds were further analyzed for the hydrogen bonds and only five compounds were found to have a favorable number of hydrogen bonds. The calculation of docking score, pharmacophore mapping and analyzing of the binding mode showed that these five compounds may act as novel inhibitors of IspE. It is noteworthy that all the five compounds are structurally diverse that allow the optimization of each compound to further enhanced it binding affinity. The 2D structures of these compounds are given in figure 1.

3.3 Binding Mode of Final Hits Compound

The docking studies shows that the final hit compounds bind into ATP binding site of the IspE with good binding affinity and having good interactions with the ATP binding site residues. The crystal structure of Mycobacterium tuberculosis with bound ATP is not available yet. So, it is important to determine the precise site for ATP in Mycobacterium tuberculosis. The IspE from Mycobacterium abcessus was co-crystalized with ATP (PDB ID 4ED4) [53]. The structural superposition of IspE from Mycobacterium tuberculosis and Mycobacterium abcessus shows that both the ATP and its stable analogous AMP-PNP bind to the same region.The final five hit compounds were found to occupy the same regions as bound by ATP and AMP-PNP in the experimental structures [53](Fig 2).

The compound 1 makes a good interaction with the active site residues. Nine hydrogen bonds were observed between compound 1 and IspE active site residues (Fig.3a). The proposed catalytic mechanism shows that Asp and Lys correspond to the Asp140 and Lys13 of IspE are important for the transfer of phosphate group [6]. The Asp act as a proton abstracting agent and Lys act to stabilize the intermediate complex. In case of present study the compound 1 blocks both the ATP and substrate binding site. The catalytic residues Lys13 and Asp140, responsible for the substrate binding, make hydrogen bonds with the compound 1 (Fig 3a). The hydroxyl group of compound 1 are involve in the hydrogen bond with the NH group of Lys13 and oxygen and hydroxyl group of Asp140. The position of the ligand is stabilized by the hydrophobic interactions of Asn15, Leu31, Leu64, Asn70, Val99 and Ala100. In addition, the Lys95, Ser257 and Gly258 make hydrogen bonds with the compound 1.The pharmacophore mapping of compound 1 show that five features are mapped by the compound 1 (Fig 3b). The hydroxyl group of compound 1 mapped the hydrogen bond donor feature (F1) and is involve in hydrogen bond with Lys13 and Asp140 as discussed above. The two nitrogen atoms of the five member ring of compound 1 mapped the two hydrogen bond acceptor features (F3 and F6). The F5 and F2 features are mapped by the oxygen and NH group of compound 1. The binding affinity calculation, pharmacophore mapping and binding mode analyses show that the predicted compound 1 may be act as a novel inhibitor of IspE that interact with both substrate and ATP binding site.

In case of compound 2, the top ranked conformation makes eight hydrogen bonds with the active site residues. The NH group of catalytic residue Lys13 makes hydrogen bond with the oxygen atom of the compound 2 (Fig 3c). The Ser257 accept hydrogen bond from the NH group of the compound 2. The pharmacophore mapping showed that NH group mapped the hydrogen bond donor feature (Fig 3d). In addition the residues Ala100, Gly101, Gly102 and Gly106 are involved in the hydrogen bonds interactions. The Leu18 and Leu64 are in hydrophobic interaction with compound 2. The figure 4b shows the mapping of pharmacophore features of compound 2.

The compound 3 binding site comprise the residues Lys13, Asn15, Leu64, Gly101, Gly102, Met103 and Ala104. Eight hydrogen bonds are observed between the compound 3 and active site (Fig 4a). The side chain of Lys13 and Asn15 make hydrogen bond with the compound 3. Similarly the backbone NH group of Gly101, Gly102, Met103 and Ala104 are involved in hydrogen bond interaction with compound 3. The compound 3 mapped the two hydrogen bond donor features along with four hydrogen bond acceptor features (Fig 4b).

The binding profile of compound 4 includes the catalytic residue Lys13 that interact with the compound 4 by making hydrogen bond (Fig 4c). The other residues such as Lys95, Pro98, Gly102, Gly105, Gly106 and Ser257 are also involved in the hydrogen bonding network. Beside hydrogen bonds, hydrophobic interactions also contribute to the stability of compound in the active site of IspE. The residue Leu31 and leu64 are involved in the hydrophobic interactions. The compound 4 mapped two hydrogen bond donor features (F1 and F2) (Fig 4d). Both features are involved in the hydrogen bonds. The F1 is involved in hydrogen bond with Ser257 while F2 is involved with the pro98 and Gly105. The compound 4 also mapped three hydrogen bond acceptor features (F4, F5 and F6). Two features F5 and F6 are involved in the hydrogen bond. The F5 make hydrogen bond with Gly105 while F6 make hydrogen bond with Gly102.

The compound 5 make nine hydrogen bonds with the active site of IspE. In case of compound 5 the catalytic reside Asp140 make hydrogen bond (Fig 4e). As discussed above, that Asp is catalytic residue and act as proton abstracting agent [6]. In case of compound 5, the Asp140 accept hydrogen bond from the NH group of compound 5. The oxygen atom of Gly105 makes two hydrogen bonds with the NH group of Gly105. The backbone NH group of Gly101, Gly102 and Met103 are involved in hydrogen bond interactions with OH group of compound 5 (Fig 4e). The Ile97, Pro98 and Val99 are in hydrogen interactions with the compound 5. In addition, the hydrophobic interactions are also present. The residues Leu18, Leu64, Leu71, Ser139 and Met226 are involved in hydrophobic interactions. The pharmacophore mapping shows that compound 5 mapped two hydrogen bond donor features (F1 and F2) and three hydrogen bond acceptor features (F4, F5 and F6) (Fig 4f). The F1 and F2 features are involved in hydrogen bond with Asp140 and Ile97, Val99 respectively. Two of the acceptor features are also involved in the hydrogen bond. The F4 makes hydrogen bond with Pro98, Val99, Gly101, Gly102 and Met103 while F6 make hydrogen bond with Gly105.

3.4 Molecular Dynamics Simulation

The docking procedure was used and the position of each compound was found in the active site of IspE. The docking results give only static interactions but in vivo the interaction process between ligand and target is dynamic in nature. Therefore, dynamic simulation was performed on each complex to check the stability of each compound in the active site of IspE. The stability of each complex was checked in term of root mean square deviation (RMSD). Figure 5 shows the RMSD graph of each complex. As the RMSD value for all the complexes is below 2 Å, it means that IspE suffered no significant structural changes during the 30 ns of MD simulation. The RMSD values increased up to 1.5 Å during the first 10 ns and then fluctuates around 1 Å for the rest of simulation. The RMSD graph shows that the all compounds are more stable. The lowest RMSD was shown by the compound 1, 2, 3 and 5. This can be attributed to the best fitting of compound 2 and 3 in the active site that make it enable to establish strong interaction with the active site of IspE. The alignment of initial (0ns) and final structure (30ns) of the compound 2 and 3 complexes (Fig 5B and C) are in consistence with the RMSD graph and support each other. It was also found that docking score and binding affinity of the compound 2 and 3 (table 1) are almost same and support the results of MD simulations.

In case of compound 1 the RMSD is also fluctuate within narrow range. The RMSD graph for compound 1 shows that it is stable during the first 20ns and then its change it geometry from bent shape to relax shape (Figure 5A). The superposition shows that compound 1 suffer a little conformational change. Due to this change, the RMSD raised but it stable during the rest of simulation. As the RMSD of compound 1 is within the range of 0.5 Å, it may be accepted as a good inhibitor.

In case of compound 5, the RMSD is stable but as compared to the compound 2 and 3, the compound 5 shows a highest RMSD. This can be attributed to the change in the geometry of compound 5 from bent shape to the relax shape during the first 15ns as shown in figure 8E and then remain stable in the relax conformation. It is interesting to observe that in the relax geometry, the compound 5 is stable in the active site and block both the substrate and ATP binding site (Fig 5E). The compound 5 may block the access to the important residues Tyr24, His25 and Tyr175 correspond to the Tyr24, His25 and Tyr181 of the Mycobacterium tuberculosis IspE that are responsible for the substrate binding [4].

In case of compound 4, the RMSD graph raise up to 1.7 Å during the 2ns and then remain stable for the rest of simulation. But during the first 2ns, the compound 4 changed its position from the active site. The figure 5D shows the change in the position of compound 4. As it changed its position, the compound 4 may not be a good inhibitor.

The binding energy analyses that driving the interaction between the IspE and the ligands were investigated. The binding energy of each ligand bound to IspE is shown in the table 2. The negative values of the ΔGBIND for all the compounds shows that these are favorable protein-ligand complexes. As shown by the table 2, the most favorable binding energy is

the Van der Waals energy for all the five compounds. As expected, the lowest binding energy was shown by the compound 2 and 3 with ΔGBIND -38.9628Kcal/mol and -34.2193Kcal/mol respectively. This can be attributing to the best binding of the compound 2 and 3 in the active site of IspE. The RMSD analysis of compound 2 and 3 supports the MMPBSA analysis. The RMSD analysis shows that compound 2 and 3 are more stable in the active site. In case of compound 1 and 5, the ΔGBIND is almost same as expected by the MD simulation analysis in figure 5. The ΔGBIND for the compound 4 is -26.4236Kcal/mol. As this value is not good as compared to the ΔGBIND of compound 1, 2, 3 and 5 therefore the compound 4 may not be a good inhibitor. In addition, the electrostatic and non-polar energy also play important role in the binding of all five compounds. Based on the ΔGBIND , compound 1,2 3 and 5 may be a potent candidates to IspE inhibitors. Therefore, the synthesis of these compound and tests in vitro and in vivo as IspE inhibitors will be interesting to corroborate our results.

IV. CONCLUSION

The non-mevalonate pathway uses seven enzymes in the synthesis of isopentenyl diphosphate (IPP) and dimethylallyl diphosphate (DMAPP) from the starting material pyruvate and glyceraldehyde-3-phosphate. In the present study the ZINC database were screened and five novel and diverse compounds were described as inhibitors of IspE. Previous studies have done, taking into account the substrate binding site. In the present study, the binding site of AMP-PNP, a stable analog of ATP, was used. The molecular docking and MD simulation found the five novel compounds that were described as inhibitor of IspE. All of the five compounds were structurally distinct as they belong to different class of compounds. The described compounds in this study possess a favorable drug like properties. So, this put forward an opportunity and state a good starting point for further optimization.

REFERENCES

[1] Comas I, Gagneux S (2009) The past and future of tuberculosis research. PLoS Pathog 5: e1000600.

[2] Davies PD (2003) The role of DOTS in tuberculosis treatment and control. Am J Respir Med 2: 203-209.

[3] Hunter WN (2007) The non-mevalonate pathway of isoprenoid precursor biosynthesis. J Biol Chem 282: 21573-21577.

[4] Tidten-Luksch N, Grimaldi R, Torrie LS, Frearson JA, Hunter WN, et al. (2012) IspE inhibitors identified by a combination of in silico and in vitro high-throughput screening. PLoS One 7: e35792.

[5] Wada T, Kuzuyama T, Satoh S, Kuramitsu S, Yokoyama S, et al. (2003) Crystal structure of 4-(cytidine 5'-diphospho)-2-C-methyl-D-erythritol kinase, an enzyme in the non-mevalonate pathway of isoprenoid synthesis. J Biol Chem 278: 30022-30027.

[6] Miallau L, Alphey MS, Kemp LE, Leonard GA, McSweeney SM, et al. (2003) Biosynthesis of isoprenoids: crystal structure of 4-diphosphocytidyl-2C-methyl-D-erythritol kinase. Proc Natl Acad Sci U S A 100: 9173-9178.

[7] Narayanasamy P, Eoh H, Crick DC (2008) Chemoenzymatic synthesis of 4-diphosphocytidyl-2-C-methyl-D-erythritol: A substrate for IspE. Tetrahedron Lett 49: 4461-4463.

[8] Beytia ED, Porter JW (1976) Biochemistry of polyisoprenoid biosynthesis. Annu Rev Biochem 45: 113-142.

[9] Edwards PA, Ericsson J (1999) Sterols and isoprenoids: signaling molecules derived from the cholesterol biosynthetic pathway. Annu Rev Biochem 68: 157-185.

[10] Boucher Y, Doolittle WF (2000) The role of lateral gene transfer in the evolution of isoprenoid biosynthesis pathways. Mol Microbiol 37: 703-716.

[11] Kuzuyama T (2002) Mevalonate and nonmevalonate pathways for the biosynthesis of isoprene units. Biosci Biotechnol Biochem 66: 1619-1627.

[12] Rohdich F, Kis K, Bacher A, Eisenreich W (2001) The non-mevalonate pathway of isoprenoids: genes, enzymes and intermediates. Curr Opin Chem Biol 5: 535-540.

[13] Lange BM, Rujan T, Martin W, Croteau R (2000) Isoprenoid biosynthesis: the evolution of two ancient and distinct pathways across genomes. Proc Natl Acad Sci U S A 97: 13172-13177.

[14] Rohdich F, Bacher A, Eisenreich W (2005) Isoprenoid biosynthetic pathways as anti-infective drug targets. Biochem Soc Trans 33: 785-791.

[15] Jomaa H, Wiesner J, Sanderbrand S, Altincicek B, Weidemeyer C, et al. (1999) Inhibitors of the nonmevalonate pathway of isoprenoid biosynthesis as antimalarial drugs. Science 285: 1573-1576.

[16] Kobayashi K, Ehrlich SD, Albertini A, Amati G, Andersen KK, et al. (2003) Essential Bacillus subtilis genes. Proc Natl Acad Sci U S A 100: 4678-4683.

[17] Freiberg C, Wieland B, Spaltmann F, Ehlert K, Brotz H, et al. (2001) Identification of novel essential Escherichia coli genes conserved among pathogenic bacteria. J Mol Microbiol Biotechnol 3: 483-489.

[18] Akerley BJ, Rubin EJ, Novick VL, Amaya K, Judson N, et al. (2002) A genome-scale analysis for identification of genes required for growth or survival of Haemophilus influenzae. Proc Natl Acad Sci U S A 99: 966-971.

[19] Shan S, Chen X, Liu T, Zhao H, Rao Z, et al. (2011) Crystal structure of 4-diphosphocytidyl-2-C-methyl-D-erythritol kinase (IspE) from Mycobacterium tuberculosis. FASEB J 25: 1577-1584.

[20] Tang M, Odejinmi SI, Allette YM, Vankayalapati H, Lai K (2011) Identification of novel small molecule inhibitors of 4-diphosphocytidyl-2-C-methyl-D-erythritol (CDP-ME) kinase of Gram-negative bacteria. Bioorg Med Chem 19: 5886-5895.

[21] Wang Q, Edupuganti R, Tavares CD, Dalby KN, Ren P (2015) Using docking and alchemical free energy approach to determine the binding mechanism of eEF2K inhibitors and prioritizing the compound synthesis. Front Mol Biosci 2: 9.

[22] Kim Y, Anderson MO, Park J, Lee MG, Namkung W, et al. (2015) Benzopyrimido-pyrrolo-oxazine-dione (R)-BPO-27 Inhibits CFTR Chloride Channel Gating by Competition with ATP. Mol Pharmacol 88: 689-696.

[23] Lee SC, Min HY, Choi H, Kim HS, Kim KC, et al. (2015) Synthesis and Evaluation of a Novel Deguelin Derivative, L80, which Disrupts ATP Binding to the C-terminal Domain of Heat Shock Protein 90. Mol Pharmacol 88: 245-255.

[24] Irwin JJ, Shoichet BK (2005) ZINC--a free database of commercially available compounds for virtual screening. J Chem Inf Model 45: 177-182.

[25] Labute P (2008) The generalized Born/volume integral implicit solvent model: estimation of the free energy of hydration using London dispersion instead of atomic surface area. Journal of computational chemistry 29: 1693-1698.

[26] Case D, Berryman J, Betz R, Cerutti D, Cheatham I, et al. (2015) AMBER 2015. University of California, San Francisco.

[27] Jorgensen WL, Chandrasekhar J, Madura JD, Impey RW, Klein ML (1983) Comparison of simple potential functions for simulating liquid water. The Journal of chemical physics 79: 926-935.

[28] Gotz AW, Williamson MJ, Xu D, Poole D, Le Grand S, et al. (2012) Routine Microsecond Molecular Dynamics Simulations with AMBER on GPUs. 1. Generalized Born. J Chem Theory Comput 8: 1542-1555.

[29] Ryckaert J-P, Ciccotti G, Berendsen HJ (1977) Numerical integration of the cartesian equations of motion of a system with constraints: molecular dynamics of n-alkanes. Journal of Computational Physics 23: 327-341.

[30] Darden T, York D, Pedersen L (1993) Particle mesh Ewald: An N· log (N) method for Ewald sums in large systems. The Journal of chemical physics 98: 10089-10092.

[31] Kouassi AF, Kone M, Keita M, Esmel A, Megnassan E, et al. (2015) Computer-Aided Design of Orally Bioavailable Pyrrolidine Carboxamide Inhibitors of Enoyl-Acyl Carrier Protein Reductase of Mycobacterium tuberculosis with Favorable Pharmacokinetic Profiles. Int J Mol Sci 16: 29744-29771.

[32] Zhou Y, Ma J, Lin X, Huang XP, Wu K, et al. (2016) Structure-Based Discovery of Novel and Selective 5-Hydroxytryptamine 2B Receptor Antagonists for the Treatment of Irritable Bowel Syndrome. J Med Chem.

[33] Miller BR, 3rd, McGee TD, Jr., Swails JM, Homeyer N, Gohlke H, et al. (2012) MMPBSA.py: An Efficient Program for End-State Free Energy Calculations. J Chem Theory Comput 8: 3314-3321.

ISSN 2348-313X (Print)
International Journal of Life Sciences Research ISSN 2348-3148 (online)
Vol. 4, Issue 2, pp: (253-262), Month: April - June 2016, Available at: www.researchpublish.com

APPENDICES

TABLES AND FIGURES:

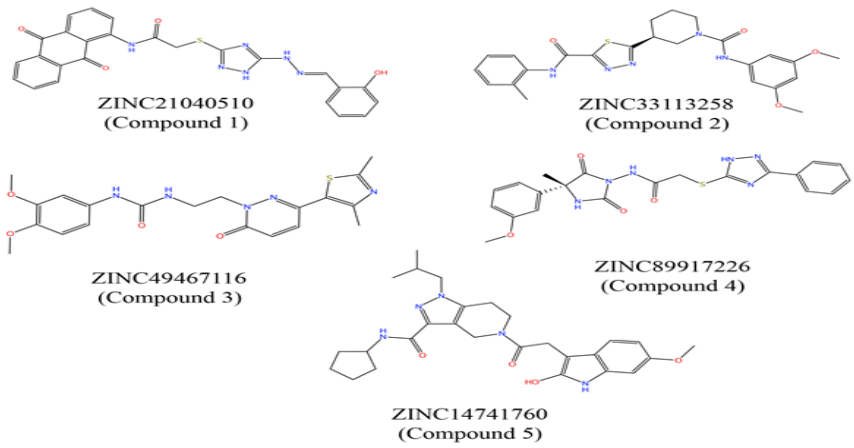

Fig.1: 2D structures of retrieved hits from ZINC database

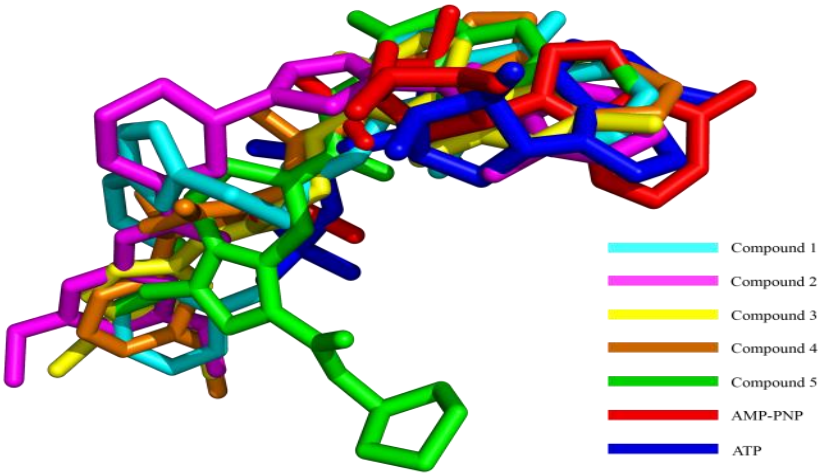

Fig.2: Superposition of hit compounds

The superposition of final hit compounds with ATP and AMP-PNP shows that all the five hits are bind to the same binding site. The colour scheme is shown inside the figure

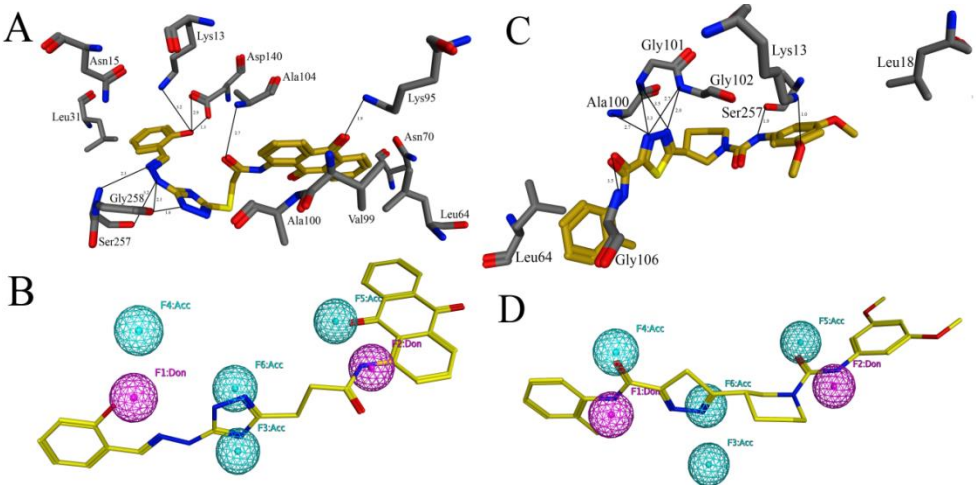

Fig.3: Binding mode and pharmacophore mapping for compound 1 and 2

ISSN 2348-313X (Print)
International Journal of Life Sciences Research ISSN 2348-3148 (online)
Vol. 4, Issue 2, pp: (253-262), Month: April - June 2016, Available at: www.researchpublish.com

The black lines show the hydrogen bonds while the number with each black line show the distance of hydrogen bond in Angstrom (A) The binding of compound 1 in the active site of IspE.. The residues Asn15, Leu31, Leu64, Asn70, Val99 and Ala100 make hydrophobic interaction with compound 1 (B) The compound 1 mapped five features. Three are hydrogen bond acceptor features and two are hydrogen bond donor features (C) The Leu18 and Leu64 are in hydrophobic interaction with compound 2 (D) compound 2 mapped five features. Two are hydrogen bond donor features while three are hydrogen bond acceptor features

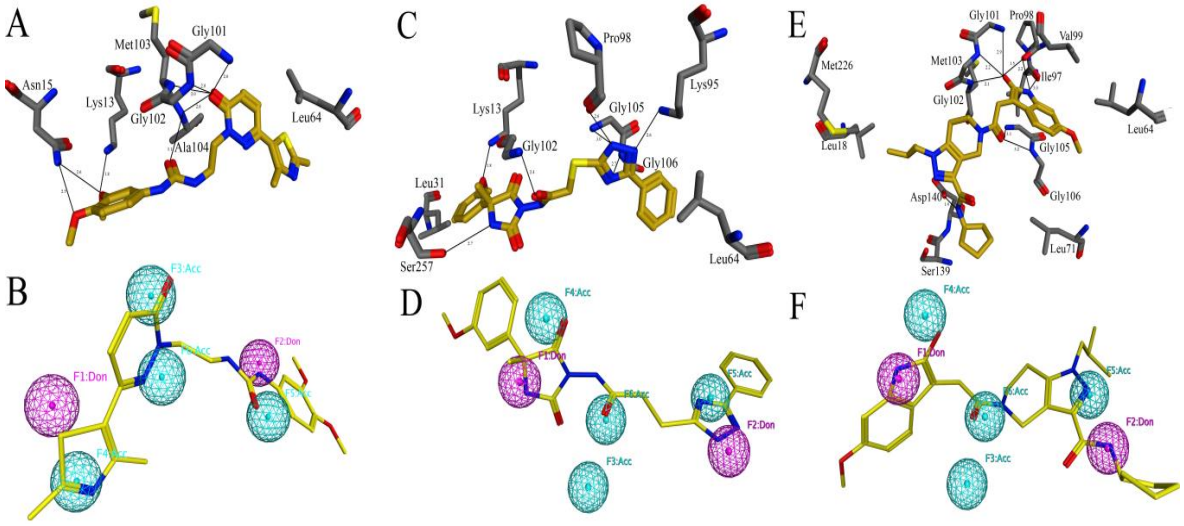

Fig.4: Binding mode and pharmacophore mapping for compound 3, 4 and 5

The black lines show the hydrogen bonds while the number with each black line show the distance of hydrogen bond in Angstrom (A) The binding of compound 3 in the active site of IspE. The Leu64 is in hydrophobic interaction with compound 3 (B) compound 3 mapped all the pharmacophore features, two hydrogen bond donor and four hydrogen bond acceptor features (C) The residue Leu31 and leu64 are involved in the hydrophobic interaction with compound 4 (D) the mapping of pharmacophoric features for the compound 4 include two hydrogen bond donor and three hydrogen bond acceptor features (E). The residues Leu18, Leu64, Leu71, Ser139 and Met226 are involved in hydrophobic interactions with compound 5 (F) the mapping of pharmacophoric features for the compound 5 include two hydrogen bond donor and three hydrogen bond acceptor features.

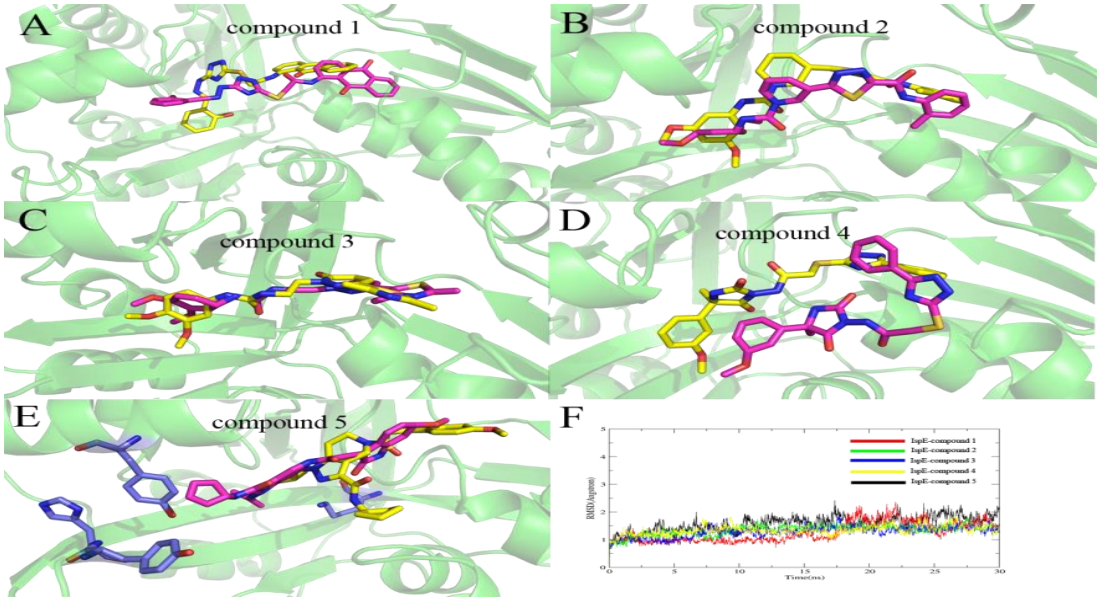

Fig.5: MD Simulation Analysis

The superposition of (A) compound 1 (B) compound 2 (C) compound 3 (D) compound 4 (E) compound 5. For all compounds the initial conformation (0ns) is shown in yellow color while the last conformation (30ns) was shown in

magenta color. (F) The RMSD graph for all the five compounds. The RMSD is shown in different color as mention in figure.

Table 1: ZINC database ID, docking score, binding affinity and drug like properties of hit compound.

Compound	ZINC ID	Docking score (MOE)	Binding affinity (kcal/mol) MOE	Binding affinity (kcal/mol) Autodock	Drug like properties
1	ZINC21040510	-8.3939	-8.35	-10.6	MW 498.5, LogP 3.46, Don 4, Acc 7
2	ZINC33113258	-7.9865	-7.88	-9.1	MW 481.5, LogP 4.52, Don 2, Acc 6
3	ZINC49467116	-7.9292	-7.85	-7.8	MW 429.5, LogP 2.70, Don 2, Acc 6
4	ZINC89917226	-7.7419	-8.20	-7.8	MW 452.4, LogP 2.38, Don 3, Acc 6
5	ZINC14741760	-7.7294	-8.70	-8.2	MW 493.6, LogP 4.06, Don 3, Acc 5
AMP-PNP		-4.83	-5.21	-7.3	

Table 2: The MMPBSA analysis of the final hit compounds of ZINC database against IspE.

Compound	ZINC ID	MM/PBSA (kcal/mol)				
		ΔG_{ELE}	$\Delta G_{VDWAALS}$	$\Delta G_{ENPOLAR}$	ΔG_{POLAR}	ΔG_{BIND}
1	ZINC21040510	-4.2676	-48.4810	-3.4120	23.6021	-32.5585
2	ZINC33113258	-2.8205	-54.4055	-4.1541	22.4174	-38.9628
3	ZINC49467116	-1.3042	-61.7743	-4.1577	43.0169	-34.2193
4	ZINC89917226	-2.5038	-38.5211	-3.3372	17.9386	-26.4236
5	ZINC14741760	-7.3624	-48.9893	-4.0165	27.7964	-32.5718